

## Experimental Evidence for Localization of Acoustic Waves in Three Dimensions

Ian S. Graham and Luc Piché

*Industrial Materials Research Institute, National Research Council, 75 De Montagne Boulevard,  
Boucherville, Québec, Canada J4B 6Y4*

Martin Grant

*Department of Physics, McGill University, Rutherford Building, 3600 University Street,  
Montréal, Québec, Canada H3A 2T8*

(Received 22 February 1990)

We present experimental evidence for localization of acoustic waves in a novel three-dimensional system. The system consists of a polymer melt solidifying by the growth of spherical semicrystalline nuclei. For sufficiently high excitation frequencies, we find renormalization of sound speed and intense absorption peaks over very narrow ranges of wave number. We generalize theory to include shear modes in the scatterers, and find that localization is consistent with our observations.

PACS numbers: 42.20.Ji, 43.20.+g, 63.20.Pw, 71.55.Jv

The propagation of waves in a medium containing randomly distributed scattering sites can lead to novel scattering phenomena. Localization<sup>1-10</sup> occurs when the diffusion constant of the wave is renormalized to zero by multiple elastic-scattering events. Anderson<sup>1</sup> introduced localization in the context of electronic systems. For classical waves,<sup>2-10</sup> localization occurs for  $l_I \gg l_E \approx \lambda$ , where  $l_I$  is the mean free path for inelastic scattering,  $l_E$  is the mean free path for elastic scattering, and  $\lambda$  is the wavelength of the incident radiation. Recently, investigations have been made of weak-localization effects close to the mobility edge, such as the enhancement of back-scattered radiation by the constructive interference of time-reversed pairs of scattering sequences.<sup>11,12</sup> This effect has been observed in several optical-scattering experiments.<sup>11-16</sup> However, strong localization has not yet been seen in light-scattering experiments, and localization effects with acoustic waves have only been confirmed for special one-dimensional systems.<sup>17</sup>

In this Letter we report the first evidence of localization phenomena for acoustic waves in a three-dimensional system. Our novel system consists of a polymer melt containing a constant number of spherical, equal-sized nuclei. During our experiment the radius  $a$  of these nuclei increases with time as the solid semicrystalline phase grows from the liquid. We excite the system by applying an ultrasonic pulse of fixed width and constant frequency. We then measure the attenuation and sound velocity through the sample, as well as the shape of the transmitted sound pulses. By performing these experiments as a function of time we are able to ultrasonically probe the system with a tunable reduced wave number  $\eta \equiv ka$ ,  $k$  being the wave number of the incident sound wave in the liquid phase. At sufficiently high frequencies we observe intense peaks in the attenuation. These peaks are narrow, spanning a limited range of scattering-site radii. We also observe renormalization of the wave velocity. These results are unexpected since the standard analysis<sup>4,6-8</sup> would not predict localization under the conditions we consider: Here, the longitudinal

sound velocity of the scatterers is *faster* than that of the medium. However, we find that, on generalizing the self-consistent theory of Condat and Kirkpatrick<sup>6,7</sup> to include shear wave excitations in the semicrystalline scatterers, localization is expected under conditions consistent with those of our experimental study. We therefore conclude that the anomalous attenuation we observe is a localization-related effect. It is not possible without further study to establish whether we are observing strong localization or precursor effects of localization, although our results are more consistent with the former.

The details of the experimental apparatus will be presented elsewhere.<sup>18</sup> The sample, a thin 0.5-cm disk, 4.0 cm in diameter, is confined between two aligned buffer rods having ultrasonic transducers at the outer ends. The buffer rods are free to move vertically to compensate for the thermal expansion of the sample, and the axial length of the assembly can be measured to within  $\pm 1 \mu\text{m}$  so that sample thickness, and hence volume, can be accurately determined. The whole assembly can be maintained at constant temperatures with a stability of  $\pm 0.1$  K. For measurements, one of the transducers is energized and provides an effective plane wave across the surface of the sample. Similarly, the second transducer, used for detection, is sensitive only to signals coherent across the transducer surface. A homodyne system is used to measure the phase of the transmitted signal with respect to the incident pulse, which allows us to measure both the attenuation and phase velocity through the sample. The data are processed to account for the acoustic properties of the buffer and the buffer-sample acoustic mismatch.<sup>18</sup>

We used a sample of isotactic polypropylene (Himont, Varennes, Canada), which has a liquid-solid transition near  $T_m = 438$  K. We anneal the liquid sample at 453 K for 20 min, and then quench to 425 K. In a separate experiment, we used a transmission polarizing microscope to visualize the evolution of the structure during solidification. We observed that (1) the nucleation centers were randomly distributed, (2) the growth was

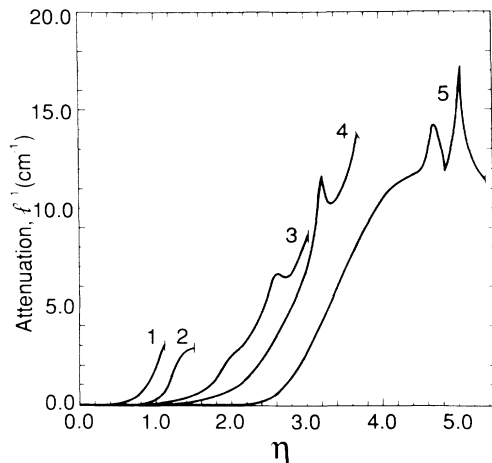


FIG. 1. Attenuation  $l^{-1}$  vs reduced wave number  $\eta \equiv ka$  for different measuring frequencies: (1) 1.75, (2) 2.50, (3) 4.88, (4) 6.00, and (5) 8.00 MHz. The curves have been truncated at the volume fraction for random close packing of spheres with radii  $a(\text{RCP}) = 125 \mu\text{m}$ .

radial such that the volume of the individual spherulite is  $\Omega = 4\pi a^3/3$ , (3) the growth was initiated simultaneously for the different spherulites and therefore their number was constant, and (4) the growth rate was constant ( $\approx 1.5 \mu\text{m}/\text{min}$ ) such that the spherulites were of uniform size. The system is consequently highly monodisperse. Making the assumption of random-close-packed (RCP) structures from the solid, we find  $a(\text{RCP}) = 125 \mu\text{m}$ , corresponding to a number density  $n \approx 5 \times 10^4/\text{cm}^3$ . Using  $a(\text{RCP})$ , our ultrasonic technique, which monitors volume, also allows us to assess the radii of the scatterers during growth. The system does not evolve over the time scale of the acoustic measurements, because we probe the system with ultrasonic longitudinal-wave pulses of duration  $\approx 6 \mu\text{sec}$ , with a rise time and fall time of  $\approx 2 \mu\text{sec}$ . We also continuously measured the attenuation and sound velocity within the sample at the characteristic frequency of the ultrasonic transducers, 1.75, 2.5, 4.88, 6.0, and 8.0 MHz.

Characteristic results for attenuation  $l^{-1}$  versus dimensionless wave number  $\eta$  are shown in Fig. 1, where  $\eta \equiv 2\pi\nu a/c$ ,  $\nu$  is the excitation frequency,  $a$  is the radius of the nuclei, and  $c$ , the velocity of sound in the fluid, is 1250 m/sec. Here the different curves are truncated at values of  $\eta$  coinciding with random close packing. Also, we have subtracted off the residual attenuation associated with the viscosity of the liquid phase,  $\approx 0.5 \text{ cm}^{-1}$ . For the semicrystalline solid, the inelastic absorption is larger,  $\sim 2 \text{ cm}^{-1}$ . However,  $l_l$  for both liquid and solid phases is still long on the scale of interparticle spacings. At excitation frequencies of 2.5 MHz and lower, we observe a slow rise and subsequent fall in attenuation of the signal as the solid phase nucleates. However, at 4.88, 6.0, and 8.0 MHz we find distinct narrow absorption peaks. The peaks lie at quite different values of  $\eta$  for

these different excitation frequencies. They are therefore not due to single-site scattering, since such peaks would lie at the same dimensionless wave number  $\eta$ , regardless of frequency. Coincident with this strong absorption we often observe sudden changes in the measured sound velocity  $c_r$  through the sample, as shown in Fig. 2(a). This provides a clear measure of the renormalization of the sound velocity.

The shape of the transmitted pulses within the absorption peak provides additional evidence of anomalous attenuation. Figure 2(b) shows shapes typical of the transmitted pulse envelopes, taken at various positions through the absorption peak, as marked in Fig. 2(a). Far from the strong-absorption regions the transmitted pulse is simply an attenuated version of the excitation pulse, with similar shape and length. However, near the absorption region the transmitted pulse becomes significantly lengthened, and, in fact, splits into two pulses: a directly transmitted pulse and a delayed pulse. The delayed pulse is not due to reverberations within the sample: It occurs too soon after the initial pulse, and, in any case, the attenuation is too high for a reverberated signal to have appreciable amplitude. We find that the position of delayed pulse is largely independent of the excitation pulse length. Thus if the incident pulse is sufficiently long, the delayed pulse becomes a "bump" on the tail of the main transmitted pulse. We note that the delayed pulse cannot arise from reradiation from excited, oscillating spheres as such a signal would be incoherent and hence undetectable by our system. We have verified that the effect remains while changing the amplitude of the incident pulse over a range of  $\pm 10 \text{ dB}$ , which rules out saturation of a resonant absorption mechanism. Finally, we note that the first absorption peak occurs below the percolation threshold for the solid phase, so it is unlikely that bulk resonances of the entire system play a role. Having ruled out these other possibilities, we therefore interpret the delayed pulse as a resonant forward-scattering mechanism, whereby the transmitted pulse is followed by an echo arising from time-reversed scattering paths in the same direction as the incident wave. This is analogous to the resonant backscattering seen in optical experiments on localization. All these results, the high attenuation in the narrow peaks, the sound renormalization, and the anomalous forward scattering can be consistently interpreted as signs of localization of sound within the sample.

Theoretical investigations of localization<sup>4,6-8</sup> typically consider systems with structureless scatterers, unlike the more complex system we have studied. In that case, localization requires the refractive index  $M = c/c_s$  to obey  $M > 1$  where  $c$  is the sound velocity in the matrix material and  $c_s$  is the sound velocity in the scatterers. Here, the velocity of sound in the solid phase  $c_s$  is  $\approx 1600 \text{ m/sec}$ , implying  $M \approx 0.78$ , so simple theories would *not* imply localization. However, the nuclei support shear modes, of velocity  $c_s' \approx 350 \text{ m/sec}$ , which we expect to

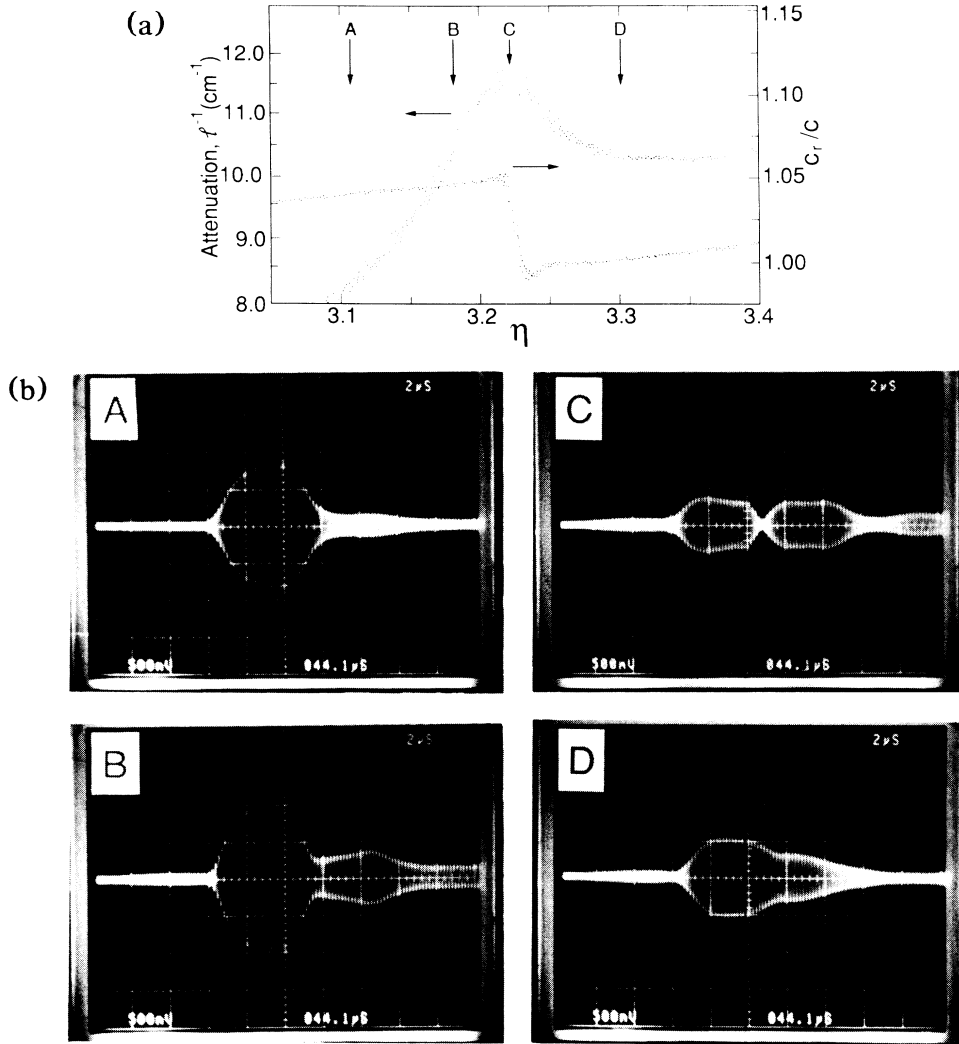


FIG. 2. (a) Attenuation  $l^{-1}$  and ratio of measured velocity to velocity in the liquid  $c_r/c$  as a function of reduced wave number  $\eta$  in the vicinity of the absorption peak for the 6.00-MHz data. (b) Photographs from oscilloscope showing shape of transmitted signals; labels *A*, *B*, *C*, and *D* refer to values of  $\eta$  indicated by corresponding labels in (a). Relative to signal *A*, the amplifier gain is up 12 dB for signal *B*, 14 dB for signal *C*, and 10 dB for signal *D*.

significantly modify the single-site scattering amplitude, giving rise to resonant effects. Thus, motivated both by the nature of our experimental system and by our observations of anomalous attenuation we have generalized the previous self-consistent localization theory due to Condat and Kirkpatrick<sup>6,7</sup> to include scatterers which support shear.

Following standard treatments<sup>19</sup> we define the incident, scattered, and internal displacement waves in terms of the two fields  $\psi$  and  $\pi$ . These fields correspond, respectively, to the longitudinal and transverse parts of the wave. We describe the incident plane wave in the negative  $z$ -axis direction by the field  $\psi_i$ , given by

$$\psi_i = \sum_{m=0}^{\infty} (-i)^{m+1} (2m+1) \frac{1}{k} j_m(kr) P_m(\cos\theta),$$

where  $k = 2\pi f/c$  is the longitudinal wave number in the

fluid phase,  $c$  is the longitudinal wave velocity in the fluid,  $j_m$  are spherical Bessel functions, and  $P_m$  are the Legendre polynomials. The outgoing scattered field  $\psi_o$  can be defined similarly. Within the scatterers there are longitudinal modes,

$$\psi_s = \sum_{m=0}^{\infty} (-i)^{m+1} (2m+1) a B_m j_m(k_s r) P_m(\cos\theta),$$

and shear modes,

$$\pi_s = \sum_{m=0}^{\infty} (-i)^{m+1} (2m+1) a C_m j_m(\kappa r) P_m(\cos\theta),$$

where  $k_s = 2\pi f/c_s$  and  $\kappa = 2\pi f/c_s'$  are the wave numbers corresponding to the longitudinal and transverse parts of the wave,  $c_s$  is the longitudinal wave velocity, and  $c_s'$  is the transverse wave velocity in the scatterers. To determine the amplitude of the scattered wave, we solve the

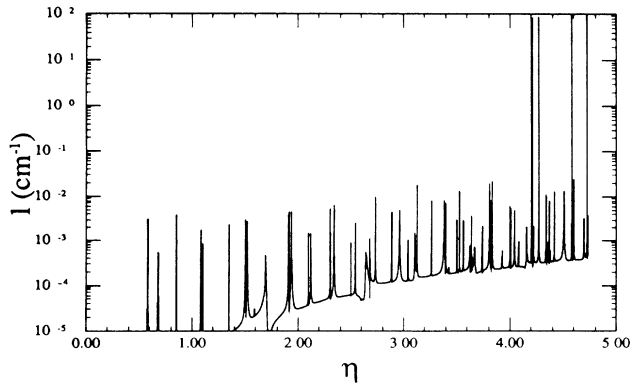


FIG. 3. Attenuation  $l^{-1}$  as a function of reduced wave number  $\eta$  as predicted by theory for an excitation frequency of 8.00 MHz. The large peaks ( $l^{-1} > 10$ ) correspond to localized states.

boundary conditions for the continuity of the displacements and stresses across the interface between the scatterer and the fluid. It is straightforward to solve for the amplitude coefficients  $A_m$ , from which the angle distribution function is given by

$$\Phi^+(\theta) = -\frac{i}{k} \sum_{m=0}^{\infty} (2m+1) A_m P_m(\cos\theta).$$

With this expression, we calculate the renormalized sound velocity and solve the self-consistent equation for the diffusion constant  $D$  in exactly the same manner as Refs. 6 and 7. The expression for the attenuation is  $l^{-1} = c/3D$ .

Characteristic theoretical results corresponding to our experimental values of number density of nuclei and  $c_s^f$  are shown in Fig. 3 for excitation frequency  $f=8$  MHz. For sufficiently high excitation frequencies, we obtain large peaks in the attenuation over a narrow range of dimensionless wave number  $\eta$ . We also obtain significant renormalization of the phase velocity through this region. These effects, which are clearly seen in our experiments, are indicative of the onset of localization. We therefore conclude that current models for classical wave localization are qualitatively consistent with our experiment, once shear-mode excitations are taken into account. Finally, our theoretical analysis suggests, quite generally, that scatterers supporting shear modes can form ideal systems for the study of acoustic localization in three dimensions. For example, broader and more prominent localized states than those in Fig. 3 are predicted to occur in systems with a larger velocity mismatch between the scatters and the matrix (for example,  $c_s/c \gtrsim 2$ ) and a large transverse velocity within the scatterer (for example,  $c_s^f/c_s \gtrsim 0.25$ ). Such situations may be possible with suitably prepared polymer systems, and clearly represent promising systems for the observation of Anderson localization.

In conclusion, we have presented the first evidence for acoustic-wave localization phenomena in a three-dimensional system. Our results demonstrate enhanced attenuation and phase-velocity renormalization within the absorption peaks, which are consistent with the predictions of localization theories. Finally we have generalized the predictions of current models for localization to include shear-mode excitation of the scatterers. This yields results which are qualitatively consistent with those of the experiment.

We thank Dik Harris, Hong Guo, and John Ström-Olsen for useful discussions and suggestions. The authors also acknowledge the technical assistance of Ginette Lessard and André Hamel. This work was supported in part by the Natural Sciences and Engineering Research Council of Canada, and by les Fonds pour la Formation des Chercheurs et l'Aide à la Recherche de la Province du Québec.

<sup>1</sup>P. W. Anderson, Phys. Rev. **109**, 1492 (1958).

<sup>2</sup>S. John, Phys. Rev. Lett. **53**, 2169 (1984).

<sup>3</sup>P. W. Anderson, Philos. Mag. B **52**, 505 (1985).

<sup>4</sup>P. Sheng and Z.-Q. Zhang, Phys. Rev. Lett. **57**, 1879 (1986).

<sup>5</sup>K. Arya, Z. B. Su, and J. L. Birman, Phys. Rev. Lett. **57**, 2725 (1986).

<sup>6</sup>C. A. Condat, J. Acoust. Soc. Amer. **83**, 441 (1988).

<sup>7</sup>C. A. Condat and T. R. Kirkpatrick, Phys. Rev. B **36**, 6782 (1987).

<sup>8</sup>C. M. Soukoulis, E. N. Economou, G. S. Grest, and M. H. Cohen, Phys. Rev. Lett. **62**, 575 (1989).

<sup>9</sup>I. Edrei, M. Kaveh, and B. Shapiro, Phys. Rev. Lett. **62**, 2120 (1989).

<sup>10</sup>Classical localization is reviewed by D. Sornette, *Acustica* **67**, 199 (1989); **67**, 251 (1989); **68**, 15 (1989).

<sup>11</sup>E. Akkermans, P. E. Wolf, and R. Maynard, Phys. Rev. Lett. **56**, 1471 (1986), and references therein.

<sup>12</sup>Y. Kuga and A. Ishimaru, J. Opt. Soc. Am. A **8**, 831 (1984).

<sup>13</sup>M. P. van Albada and A. Lagendijk, Phys. Rev. Lett. **55**, 2692 (1985); M. P. van Albada, M. B. van der Mark, and A. Lagendijk, Phys. Rev. Lett. **58**, 361 (1987).

<sup>14</sup>P.-E. Wolf and G. Maret, Phys. Rev. Lett. **55**, 2696 (1985).

<sup>15</sup>S. Etemad, R. Thompson, and M. J. Andrejco, Phys. Rev. Lett. **57**, 575 (1986); S. Etemad, R. Thompson, M. J. Andrejco, S. John, and F. C. MacKintosh, Phys. Rev. Lett. **59**, 1420 (1987).

<sup>16</sup>M. Kaveh, M. Rosenbluth, I. Edrei, and I. Freund, Phys. Rev. Lett. **57**, 2049 (1986); I. Edrei and M. Kaveh, Phys. Rev. B **35**, 6461 (1987).

<sup>17</sup>C. H. Hodges and J. Woodhouse, J. Acoust. Soc. Amer. **74**, 894 (1983); S. He and J. D. Maynard, Phys. Rev. Lett. **57**, 3171 (1986).

<sup>18</sup>L. Piché (to be published).

<sup>19</sup>R. Truell, C. Elbaum, and B. B. Chick, *Ultrasonic Methods in Solid State Physics* (Academic, New York, 1969).

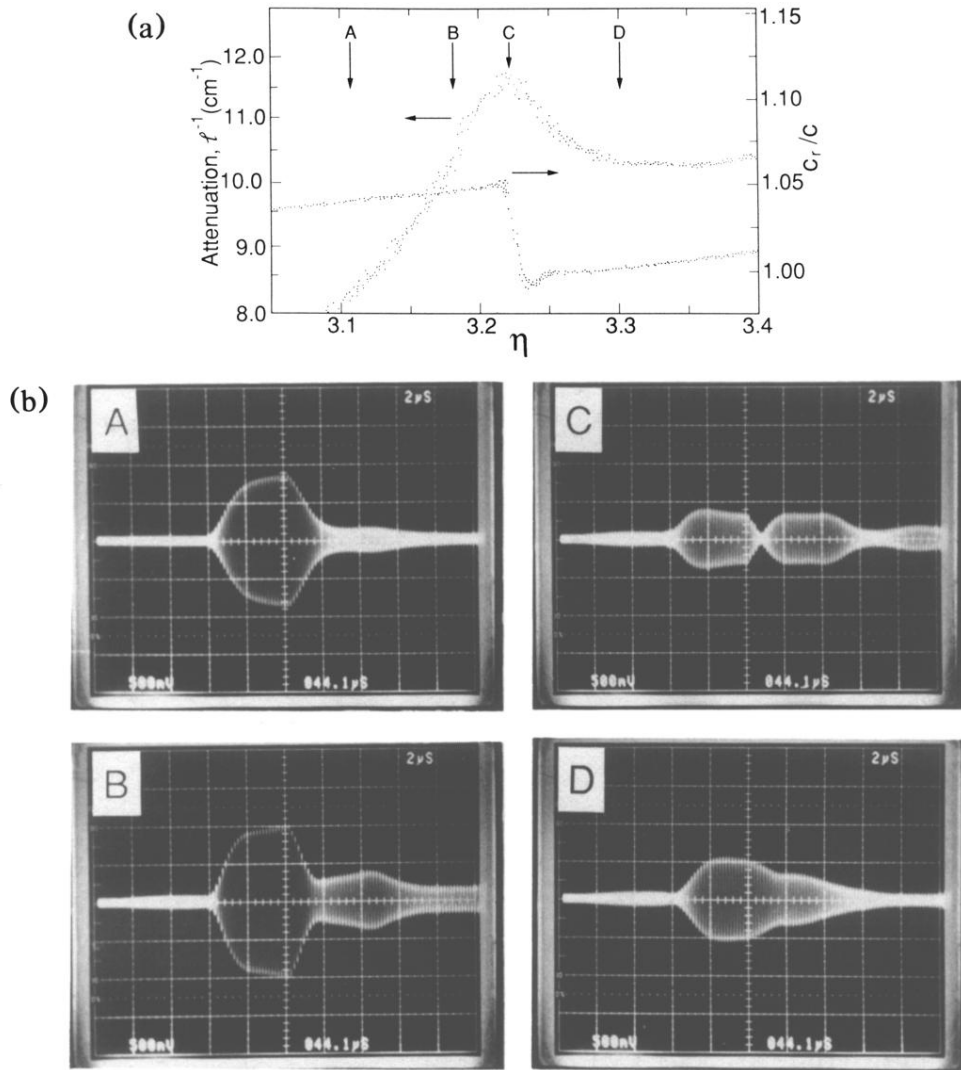


FIG. 2. (a) Attenuation  $l^{-1}$  and ratio of measured velocity to velocity in the liquid  $c_r/c$  as a function of reduced wave number  $\eta$  in the vicinity of the absorption peak for the 6.00-MHz data. (b) Photographs from oscilloscope showing shape of transmitted signals; labels *A*, *B*, *C*, and *D* refer to values of  $\eta$  indicated by corresponding labels in (a). Relative to signal *A*, the amplifier gain is up 12 dB for signal *B*, 14 dB for signal *C*, and 10 dB for signal *D*.